Ukrainian Journal of Physical Optics
ISSUE 1
2026

Optical and Morphological Features of Silver Species Formed in LiB_3O_5:Ag Glass by Thermal and Laser Treatment

V.T. Adamiv [1,*], Ya.V. Burak [1], I.M. Teslyuk [1], R.V. Gamernyk [2], V.I. Horchynskyi [3], O.M. Yaremko [3]

[1] O.G. Vlokh Institute of Physical Optics of the Ivan Franko National University of Lviv, 23 Dragomanov St., Lviv, 79005, Ukraine
[2] Department of Experimental Physics, Ivan Franko National University of Lviv, 8 Kyryla and Methodiya St., 79005, Lviv, Ukraine
[3] National University "Lviv Polytechnic", 12 Stepan Bandera St., Lviv, 79013, Ukraine
*Corresponding author: adamiv@ifo.lviv.ua

Received: 21.01.2026

Abstract. The morphology and optical properties of Ag nanoparticles (Ag NPs) in LiB_3O_5:Ag (0.1 mol.%) glass samples formed by thermal annealing in air and vacuum, as well as under the influence of high-power laser radiation, were studied. It was found that most Ag NPs formed by thermal annealing in air have an almost spherical shape with Ranging from 20 to 100 nm, and a significant part of the surface of the samples annealed in vacuum is covered with Ag NPs that are highly distorted relative to a spherical shape, with sizes between 100 and 200 nm, and are in electrical contact with each other. Lorentzian decomposition of the recorded absorption spectra revealed three component absorption bands—at 241 nm, 367 nm, and 426 nm—of which only the band at 426 nm is associated with the plasmon resonance of Ag NPs located in the near-surface layer of the sample; the other two bands at 241 nm and 367 nm are related to Ag^+ ions and Ag_2^+ aggregates in the bulk of the glass. After treatment with laser radiation at λ = 405 nm and a power of 1.0 W, the surface of the glass sample is covered with a non-continuous film of metallic Ag, over which lamellar dendrites with a width of 100–240 nm and a length of 1–5 μm are observed. In the absorption spectrum, bands at 368 nm and 820 nm caused by surface plasmon resonance are recorded, with the first band representing the non-continuous Ag film, while the second is most likely associated with dendrites of metallic Ag.

Keywords: borate glasses, Ag nanoparticles, plasmon resonance, LiB_3O_5:Ag
UDC: 535.8, 538.9
DOI: 10.3116/16091833/Ukr.J.Phys.Opt.2026.01122

1. Introduction

In recent decades, interest has grown significantly in nanocomposite materials, especially those based on metallic nanoparticles (NPs) in dielectric media. This interest stems from the substantial influence of metallic NPs on the linear and nonlinear susceptibilities of the corresponding dielectric medium—the matrix [1,2] – and on processes of radiative recombination [3]. Noble metal NPs (Au and Ag) attract considerable attention because of their unique optical properties in the near UV and visible spectral ranges [4]; consequently, nanocomposites based on these are already being used practically as biosensors due to plasmon resonance [5].

Often, dielectric media for the formation of metallic NPs are glass matrices of various compositions [6], for example, Co NPs in borosilicate glass [7], Au NPs in bismuth borate glasses [8], or in silicate glasses [9]. In recent years, Ag NPs on the surface and in the bulk of glass matrices based on borates have attracted particular attention, in particular, in borate

glasses - $Li_2B_4O_7$ [10], $LiCaBO_3$-Ag_2O and $LiCaBO_3$-Gd_2O_3-Ag_2O [11], CaB_4O_7-Gd_2O_3-Ag_2O [12], $LiKB_4O_7$–Ag_2O and $LiKB_4O_7$–Ag_2O–Gd_2O_3 [13]. In such nanocomposites based on the aforementioned borate glasses with Ag NPs, clear peaks in the optical absorption spectra were found, which are associated with surface and near-surface plasmon resonance [10–13]. It was also found that in the presence of Ag NPs in these borate glasses, a significant increase in nonlinear coefficients is observed; in particular, the nonlinear refractive index n_2 sharply increases in absolute value by 4 orders of magnitude. Accordingly, the authors of [10] suggested that doped $Li_2B_4O_7$:Ag glass with an Ag NP interface layer can be used as an efficient optical limiter, which requires high nonlinear refractive-index materials.

Therefore, borate glasses are considered the most promising for forming Ag NPs on both the surface and inside the sample. This is due to their unique structure. Almost all borates have a framework structure built from borooxygen complexes, which are formed by strong covalent B–O bonds and act as anions. Metal cations are located in the gaps between these complexes and, connected by weaker ionic bonds, mainly serve as charge compensators in the borate crystal lattice. This includes borates with both alkaline-earth and alkali cations, such as $Li_2B_4O_7$ [14], $LiKB_4O_7$ [15], LiB_3O_5 [16], and CaB_4O_7 [17].

During the formation of borate glass, the framework structure of borooxygen complexes is broken down, meaning the long-range order between these complexes no longer exists. However, the complexes themselves are preserved because of the strength of the B – O covalent bonds. As a result, the structure of borate glass is made up of randomly arranged borooxygen complexes, with metal ions located in the voids between them. This type of structure allows Ag^+ ions to be relatively easily reduced to neutral Ag^0 atoms through exchange with borooxygen complexes and enables them to move easily through the glass structure. This facilitates the formation of Ag NPs both inside the bulk and on the surface of borate glass samples during thermal treatment.

Our practical experience in forming Ag NPs in $Li_2B_4O_7$ [10] and $LiKB_4O_7$ [12] confirmed the promising potential of borate glasses based on alkaline earth metals, especially lithium tetraborate [10]. However, researchers have overlooked lithium triborate (LiB_3O_5), which has a Li/B ratio of 1/3, compared to 1/2 in tetraborates. Therefore, it is likely that in LiB_3O_5:Ag glass, the reduction of Ag^+ ions to neutral Ag0 atoms occurs more actively, leading to more active formation of Ag NPs. This work focuses on studying Ag NPs in glass samples LiB_3O_5:Ag (0.1 mol.%), produced through annealing in air, vacuum, and under laser irradiation, using the optical absorption method.

2. Experimental

The solid-state reaction method was used to synthesize the lithium triborate compound. Lithium carbonate Li_2CO_3 and boric acid H_3BO_3 from Merck, with a purity of at least 99.99%, served as the starting materials. The reagents were mixed in specific ratios according to the phase diagram of borate compounds [18]. The mixture was placed in a ceramic crucible and slowly heated in a resistive furnace to a temperature of 700°C (973 K) to ensure the reaction was completed successfully:

$$Li_2CO_3 + 6H_3BO_3 \rightarrow 2LiB_3O_5 + CO_2 + 9H_2O.$$

As a result, the compound LiB_3O_5 with T_{melt} = 1107 K was obtained. Then, $AgNO_3$ was added to the powder at a concentration of 0.1 mol.% Ag, and the mixture was thoroughly ground in an agate mortar.

The glass was prepared by melting the material in a platinum crucible under air at 1200 K (approximately 100 K above T_{melt}) and was held for at least 1 h to homogenize the melt. After that, the melt was poured onto a metal plate at room temperature. Samples in the form of plates with a thickness of 1.5 mm were cut from the resulting glass, and their surfaces were ground and polished.

Since the main method of forming metal nanoparticles in glasses is associated with the decomposition of a supersaturated solid solution of a neutral metal in the matrix, the key stage of this method is the process of reducing the metal to a neutral state in the glass matrix. For this purpose, heat treatment is typically used. For the formation of Ag NPs in our LiB_3O_5:Ag glass samples, annealing was used at a temperature of 723±5 K for 2 h in an air atmosphere or in a vacuum of $<10^{-4}$ mm Hg with a titanium getter. To conduct an experiment on the formation of Ag NPs under continuous exposure to laser radiation for one hour, a CW Rui Diao laser with a power of 1.0 W, a wavelength of 405 nm, and a beam diameter on the sample surface of 5 mm (15 W/cm^2) was used.

The transmission spectra were measured on a setup based on the MDR-23 monochromator and a personal computer. A halogen incandescent lamp served as the light source, and the receiver was an FEP-79 photomultiplier tube operated in quantum-counting mode, which ensured linear signal registration over the range 10^2-10^6.

The surface morphology of LiB_3O_5:Ag glass samples was studied on an electron microscope of the FEI brand - Versa 3D electron microscope (Germany). X-ray studies were performed on an AERIS Research X-ray diffractometer, Malvern Panalytical.

3. Results and discussion

Silver in molten LiB_3O_5 at a temperature of 1200 K is present in the form of Ag^+ ions, replacing Li^+ ions, which has been experimentally confirmed for $Li_2B_4O_7$:Ag single crystals [19]. However, it turned out that although Ag^+ ions occupy mainly the nodes of the LiB_3O_5 crystal lattice instead of Li^+ ions, some of the Ag^+ ions are located in the internode sites. And in [20], it is reported that when the concentration of silver in the $Li_2B_4O_7$ borate melt increases, it begins to reduce to Ag^0 and coagulate into nanoparticles, which are then captured by the growing crystal. That is, at high silver concentrations in melts, Ag nanoparticles can form even within borate single crystals.

In borate glasses, such processes of reduction of Ag^+ to Ag^0 with subsequent coagulation can occur much more intensively, especially under the influence of factors that promote the reduction of Ag^+ ions. This was demonstrated in [21], where after γ-irradiation in the glass LiB_3O_5:Ag neutral molecular clusters $(Ag)_n$ (n = 2-4) and even molecular ions were detected Ag_n^{m+}.

As our experience has shown, one of the effective factors contributing to the reduction of Ag^+ ions in borate glasses is heat treatment, particularly when annealing is carried out in a reducing atmosphere [10-13]. For example, the process of forming Ag NPs in borate glass $Li_2B_4O_7$:Ag [10] during annealing in vacuum occurs by reducing silver ions Ag^+ near the surface according to a process that can be written as $Ag_2O \rightarrow 1/2O_2\uparrow + 2Ag^0$. At elevated temperatures, neutral oxygen atoms leave the sample surface and enter the vacuum, while neutral Ag^0 atoms remain near the surface and can quite easily migrate along the framework structure of borate glass, with the subsequent formation of Ag NPs on its surface and in the bulk. Because the concentration of Ag^+ ions near the surface decreases during this process, their supply to the surface layer arises from diffusion of Ag^+ ions from the sample volume

toward the surface until dynamic equilibrium is reached. Apparently, the formation of Ag NPs in the borate glass LiB_3O_5:Ag will occur by a similar mechanism.

The result of the above-described process during annealing of LiB_3O_5:Ag (0.1 mol.%) glass samples at a temperature of 723±5 K for 2 h can be clearly seen in Fig. 1. As can be seen in the photo, the sample annealed in air (Fig. 1a) has a yellowish tint, while the one annealed in vacuum with a getter has a grayish color (Fig. 1b).

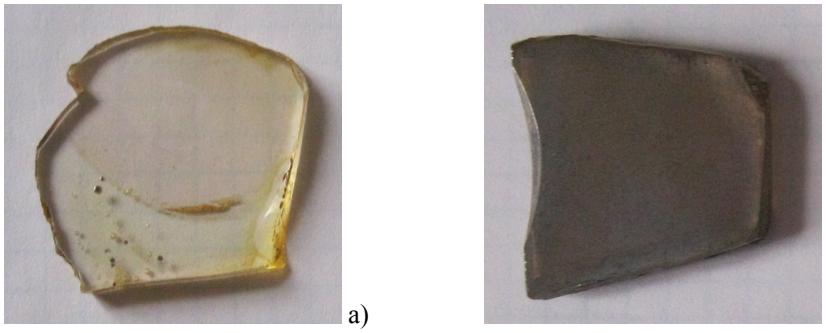

a) b)

Fig. 1. LiB_3O_5:Ag (0.1 mol.%) samples after annealing at 723±5 K for 2 h in air (a) and in vacuum (b).

This clearly confirms that in LiB_3O_5:Ag (0.1 mol.%) samples, the processes of Ag^+ reduction to Ag^0 followed by coagulation occur much more intensively during annealing in a vacuum with a getter than during annealing in air.

Studies conducted on an atomic force microscope (AFM) showed that the surface of the samples is covered with Ag NPs (Fig. 2). Moreover, if in the sample annealed in air, the Ag NPs on the surface are almost spherical in shape with sizes in the range of 20–100 nm (Fig. 2a), the surface of samples annealed in a vacuum was covered with Ag nanoparticles with sizes ranging from 100 to 200 nm and slightly distorted in relation to the spherical shape (Fig. 2b).

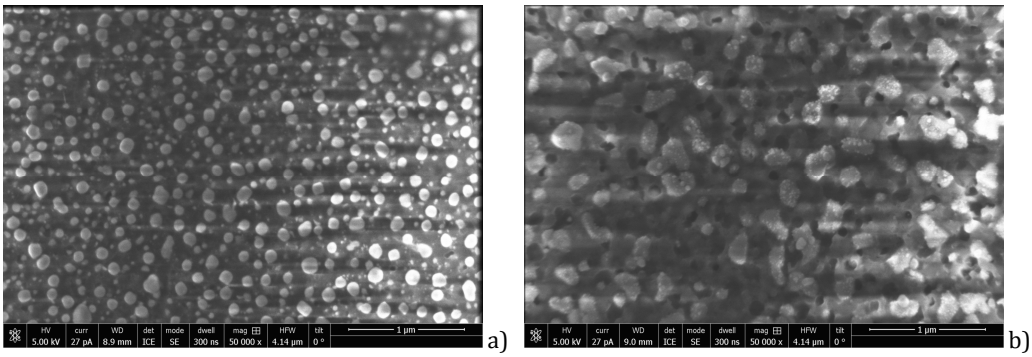

a) b)

Fig. 2. AFM image of Ag NPs on the surface of LiB_3O_5:Ag (0.1 mol.%) glass after annealing at 723±5 K for 2 h in air (a) and in vacuum (b).

As a rule, the presence of metal NPs in dielectric matrices is accompanied by the appearance of characteristic plasmon bands in their optical absorption spectra [22]. Plasmonic absorption in metal NPs is caused by the oscillatory motion of free electrons excited by the electromagnetic field of a light wave in the confined volume of a metal nanoparticle. For this, metal NPs in a dielectric matrix must not contact each other so that electrons can move only inside the nanoparticle with the formation of a dipole. The approximation of the light wave frequency to the natural frequency of such an electric dipole leads to the occurrence of resonance processes, accompanied by the appearance of additional plasmon bands in the absorption spectra of such

nanocomposite materials. Moreover, it has been proven that spherical metal NPs of the same radius have a single band of plasmon resonance, which shifts to the long-wave region with an increase in particle radius [6].

To detect the plasmonic absorption of Ag NPs in the annealed samples of LiB_3O_5:Ag (0.1 mol.%), optical absorption spectra were recorded in the range of 220 – 800 nm. As a result, Fig. 3 shows the difference absorption spectra of the samples of LiB_3O_5:Ag (0.1 mol.%) before and after annealing at a temperature of 723±5 K for 2 h in air and in vacuum.

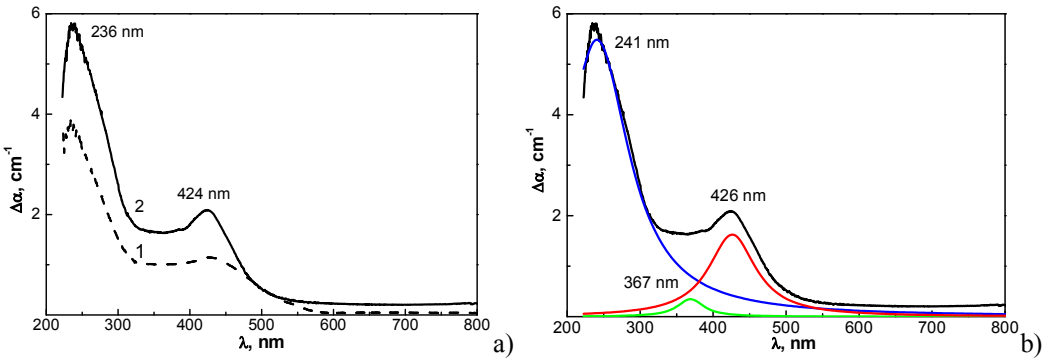

Fig. 3. Difference absorption spectra of LiB_3O_5:Ag (0.1 mol.%) samples before and after annealing at a temperature of 723±5 K in an air atmosphere – 1 and in vacuum – 2 (a); Lorentzian decomposition (color curves) of the spectrum 2 – (b).

As shown in Fig. 3a, the recorded absorption spectra clearly exhibit two maxima at 236 nm and 424 nm for both LiB_3O_5:Ag (0.1 mol.%) samples: annealed in air (spectrum 1) and annealed in vacuum (spectrum 2). These two spectra differ only in the intensity of the maxima, and, as expected, the maxima for the sample annealed in vacuum are much more intense than those for the one annealed in air. However, the shape of curve 2 indicated the possibility of its complex nature, which was confirmed by the decomposition of this spectrum into Lorentzian components (Fig. 3b). As can be seen from Fig. 3b, the recorded absorption spectra actually have 3 components: 241 nm, 367 nm, and 426 nm.

Analysis of the obtained results shows that only the 426 nm absorption band can be responsible for plasmon resonance, while the 241 nm and 367 nm absorption bands, in our case, cannot be associated with plasmon resonance, because as shown in [23], with increasing Ag NPs size, the position of the absorption bands shifts to the long-wavelength side, and not vice versa.

An important question is the location of the Ag NPs responsible for the 426 nm plasmon band. As can be seen from the AFM photograph (Fig. 2), the surfaces of the samples are covered with a continuous layer of Ag NPs of various sizes, as a result of which the Ag nanoparticles are in electrical contact with each other. Whereas, to obtain a pure plasmon resonance, it is necessary for Ag NPs to be at a distance of >20 nm [24]. That is, the Ag NPs that we see in the AFM photographs (Fig. 2) are not involved in the appearance of the 426 nm plasmon band. This means that the Ag NPs responsible for the 426 nm plasmon band are located beneath these visible surface layers of Ag NPs in the near-surface layer of the dielectric medium of the glass LiB_3O_5:Ag matrix. Moreover, according to the results of studies of the dispersion of the refractive index n of LiB_3O_5 glass in [25], its dielectric permittivity can be estimated as $\varepsilon_m = n^2$ for λ = 426 nm, i.e., ε_m = 2.4. If we apply the Fröhlich resonance condition for resonance in a metallic spherical nanoparticle $\varepsilon = -2\varepsilon_m$ (where ε is the dielectric

permittivity of the metallic nanoparticle), which describes the condition that is fulfilled when the frequency of the incident light corresponds to the collective oscillation of free electrons in the nanoparticle, leading to strong absorption and scattering of light at this frequency [26] we can also determine the dielectric permittivity of our Ag NPs in the matrix of the LiB_3O_5:Ag (0.1 mol%) surface layer: $\varepsilon = -2\varepsilon_m = -2\times2.4 = -4.8$. This value of ε correlates quite well with the values of the real and imaginary parts of the complex dielectric permittivity of noble metals, in particular Ag, in work [27].

As for the sizes of Ag NPs in the near-surface layer of the matrix, which are responsible for the 426 nm plasmon band, an attempt was made to use the known formula for Ag NPs of regular spherical shape $R = V_F/\Delta\omega$, where V_F is the Fermi velocity, which for metallic silver is 1.39×10^6 m/s [28], and $\Delta\omega$ is the half-width of the plasmon absorption band [29]. After calculating R using this formula for the 426 nm plasmon band, we obtained an effective optical radius of R=1.7 nm for Ag NPs, which is implausibly small for Ag nanoparticles in a glass LiB_3O_5:Ag matrix. Indeed, as shown by theoretical calculations for spherical Ag NPs [30] and experimental observations by the authors of the work [31], the plasmon absorption band in the ~400 nm region for Ag NPs of regular spherical shape is characteristic of Ag nanoparticle sizes at least an order of magnitude larger, i.e., R >17 nm. This difference in R values can be explained by assuming that the spherical shape of Ag NPs in our case is significantly distorted. This was well demonstrated by the authors of the work [30] for spheroid-shaped Ag NPs. That is, even small deviations of Ag NPs from the regular spherical shape lead to a shift in the absorption band. Thus, it is quite plausible that in our case, the shape of Ag NPs in the glass LiB_3O_5:Ag matrix is that of distorted spheres, which collectively leads to a broadening of the plasmon absorption band. And since the half-width of the absorption band $\Delta\omega$ is in the denominator ($R=V_F/\Delta\omega$), the use of this formula for calculating the radius in our case of Ag NPs is incorrect, as it gives very low values of R.

Although the absorption bands at 241 nm and 367 nm cannot be associated with plasmon resonance in Ag NPs, as we have seen above, their appearance is definitely related to Ag impurities. This is confirmed by the results of our previous studies on LiB_3O_5:Ag (1.0 mol.%) glass, in which we observed an absorption band in the 230–240 nm region [21]. In this work, this absorption band was associated with the formation of Ag^0 photoluminescence centers during γ-irradiation. If we now assume that annealing of LiB_3O_5:Ag (0.1 mol.%) glass samples in air, and especially in vacuum, is accompanied by a similar process of Ag^+ reduction to Ag^0, but irreversible unlike γ-irradiation due to oxygen loss, then the appearance of a 241 nm absorption peak in the difference spectrum becomes understandable (Fig. 3). In this process, the concentration of Ag^+ ions actually decreases, and accordingly, the intensity of the 241 nm peak decreases. That is, ions in the structure of LiB_3O_5:Ag (0.1 mol.%) are clearly responsible for this absorption band. The interpretation of the detected weak absorption band at 367 nm is somewhat more complex. Here, we can refer to the results of studies by authors [32,33] on the formation and luminescent properties of Ag-doped glasses. Given the tendency of silver atoms to coagulate, they suggested linking such weak absorption bands in the 300 – 400 nm range with Ag_m^{n+} aggregates. Therefore, we believe that, with a high degree of certainty, our weak absorption band at 367 nm can be explained by the formation of such aggregates with small values of m and n, for example, m = 2 and n = 1 (Ag_2^+) during the annealing of LiB_3O_5:Ag (0.1 mol.%) glass samples.

Ag NPs were also formed by laser annealing a selected area of the LiB_3O_5:Ag sample with a continuous wave laser beam with a power of 1.0 W and a wavelength of 405 nm, which is exactly in the region of the plasmon absorption band of 350 – 500 nm of LiB_3O_5:Ag glass (0.1 mol.%). The AFM image of the surface of the LiB_3O_5:Ag glass sample (0.1 mol.%) after laser irradiation for 1 h is shown in Fig. 4a.

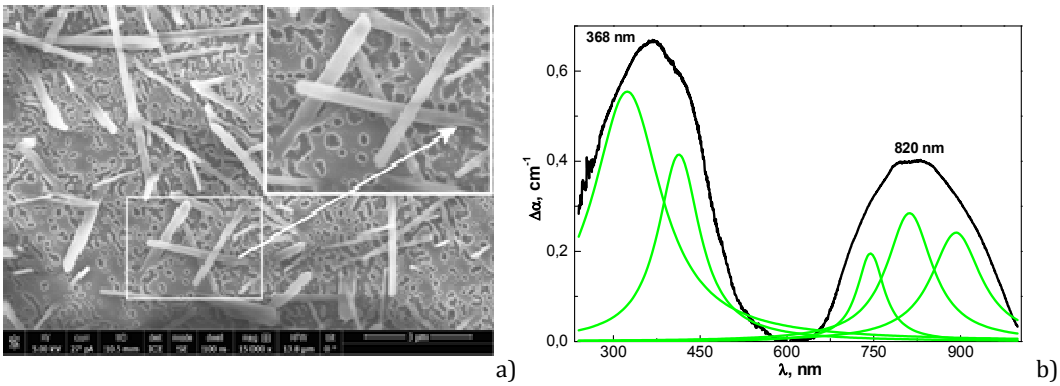

Fig. 4. (a) AFM image of Ag NPs on the surface of LiB_3O_5:Ag (0.1 mol.%) glass after laser irradiation: (b) difference absorption spectrum – before and after laser irradiation. (λ = 405 nm, beam power 1.0 W, time 1 h, beam diameter on the sample surface 5 mm. The Lorentzian decomposition is shown by the color curves.

As can be seen from the AFM image, the surface of the sample is covered with a discontinuous film of metallic Ag, above which lamellar dendrites with a width of 100–240 nm and a length of 1–5 μm are observed at an angle to the sample surface. The fact that the film and dendrites consist of metallic Ag is confirmed by the diffractogram of the laser-irradiated area of the sample (Fig. 5).

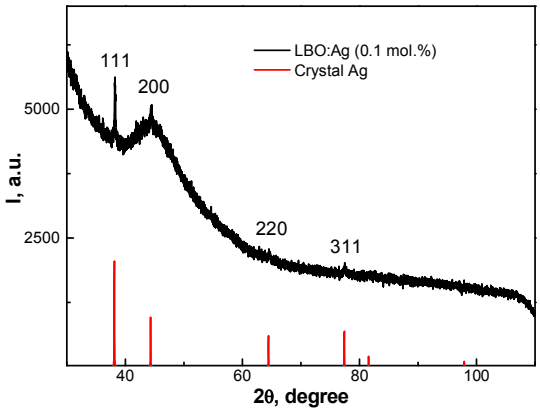

Fig. 5. Diffractogram of the sample of LiB_3O_5:Ag (0.1 mol.%) glass after laser irradiation in comparison with the diffractogram of crystalline silver.

The appearance of dendrites after laser irradiation of LiB_3O_5:Ag glass is quite unexpected. The inset in Fig. 4a shows an enlarged area of the sample surface, where it is clearly visible that the nucleation centers of these dendrites are located in the Ag film itself. This means that the dendrites separate silver nanocrystals, and additional evidence that the film with dendrites consists of metallic Ag is the fixation of plasmon resonance in the optical absorption spectrum (Fig. 4b). Fig. 4b shows the difference spectrum (before and after laser irradiation) of plasmon absorption, where two broad absorption bands of low intensity with maxima at 368 nm and 820 nm are clearly visible.

At first glance, these bands appear to be complex in nature, so they were decomposed into Lorentzian components. In particular, the first band at 368 nm is decomposed into two bands with maxima at 324 nm and 420 nm, while the second band at 820 nm is decomposed into three component bands with maxima at 743 nm, 812 nm, and 893 nm.

To interpret our results, we used the findings of detailed experimental studies of plasmon resonance in ultrathin Ag films reported in [34] and theoretical studies of the influence of the shape and size of Ag NPs on the position and shape of plasmon absorption bands reported in [30]. Thus, Bolesta I.M. et al. [34] recorded a broad plasmon absorption band with a maximum at ~ 480 nm in the spectrum of an ultrathin Ag film, which is due to the collective motion of free charge carriers confined to the surface of metal clusters. Moreover, a thickness dependence of the plasmon spectrum was revealed due to the strong inhomogeneous broadening of the absorption band as a result of an increase in the number and size of clusters, the deviation of their shape from spherical, and the electrodynamic interaction of clusters in the light wave field.

The authors of [30], in particular, investigated the behavior of plasmon resonance on Ag NPs in the form of a prism with an edge of 100 nm and a thickness of 16 nm. As a result, they found that the plasmon absorption band should lie in the 800 nm region. Moreover, even slight changes in the size and shape of the prisms lead to a noticeable shift in the position of the absorption band maximum.

Therefore, taking into account the results of the above-mentioned works [30,34], we can propose the following hypothetical interpretations of our results of laser treatment of the surface glass LiB_3O_5:Ag (0.1 mol.%): 1) the entire broad band of 368 nm corresponds to the plasmon resonance of the discontinuous Ag metal film, as interpreted in [34]; 2) but if we assume that this 368 nm band actually consists of two bands, 324 nm and 420 nm, then considering that their positions almost exactly coincide with the positions of the 367 nm and 426 nm bands obtained when decomposing the plasmon absorption band (Fig. 3b) on LiB_3O_5:Ag samples annealed in a vacuum, then similarly, the 324 nm component band may be associated with Ag_m^{n+} aggregates, and the 420 nm component band with Ag NPs in the form of distorted spheres in the near-surface layer of the glass sample; 3) the absorption band at 820 nm is most likely associated with metal Ag dendrites. Moreover, considering that the thickness of dendrites is most likely not a constant value but varies within a few nanometers, the broad 820 nm band is formed by the superposition of plasmon absorption in each individual dendrite. This is indicated by the decomposition of this band into three components (Fig. 4b).

4. Conclusions

Studies on AFM and optical properties of Ag NPs in LiB_3O_5:Ag glass samples (0.1 mol.%) formed by thermal annealing in air and vacuum, as well as under the influence of powerful laser radiation, showed:

- the bulk of Ag NPs formed by thermal annealing in air atmosphere have an almost spherical shape with R in the range of 20–100 nm, and the surface of the samples annealed in vacuum is covered with Ag NPs very distorted with respect to the spherical shape with sizes in the range of 100 – 200 nm: these Ag NPs are in electrical contact, therefore, plasmon resonance was not observed by us;
- in the recorded absorption spectra of samples annealed both in air and in vacuum, two absorption bands at 236 nm and 434 nm are clearly distinguished in both samples, differing in the intensity of the maxima (for those annealed in vacuum, the intensity is

significantly higher); Lorentzian decomposition of this absorption spectrum revealed 3 component absorption bands – 241 nm, 367 nm and 426 nm, of which only one band at 426 nm is associated with the plasmon resonance on Ag NPs which are located in the near-surface layer of the sample; the other two bands at 241 nm and 367 nm are associated with Ag^+ ions (241 nm) and Ag_2^+ aggregates (367 nm) in the glass volume;

– the surface of the sample after laser treatment is covered with a discontinuous film of metallic Ag, over which lamellar dendrites with a width of 100–240 nm and a length of 1–5 μm are observed (ASM image); analysis showed that the absorption band at 368 nm is caused by surface plasmon resonance, while the absorption band at 820 nm is most likely associated with the observed dendrites of metallic Ag.

Funding. Ministry of Education and Science of Ukraine, projects #0124U000979 and #0124U000826.

Conflict of interest. Authors declare no conflict of interest.

Reference

1. Markel, V. A., Poliakov, E. Y., & Shalaev, V. M. (1996). Small-particle composites. II. Nonlinear optical properties. *Phys. Rev.*, *B53*, 2437-2449.
2. Shalaev, V. M. (1996). Electromagnetic properties of small-particle composites. *Phys. Rep.*, *272*, 61.
3. Blanco, L. A., & Garcia de Abajo, F. J. (2004). Spontaneous emission enhancement near nanoparticles. *J. Quant. Spectr. Rad. Transf.*, *89*, 37-42.
4. Nedyalkov, N., Koleva, M. E., Nikov, R. G., Stankova, N. E., Iordanova, E., Yankov, G., Aleksandrov, L., & Iordanova, R. (2019). Tuning optical properties of noble metal nanoparticle-composed glasses by laser radiation. *Appl. Surf. Sci.*, *463*, 968-975.
5. Watzky, M. A., & Ethridge, A. J. (2025). Growth-Based Analyte and Bioanalyte Sensing Applications Using Noble Metal Nanoparticles: Effect of Nanoparticle Growth on the Localized Surface Plasmon Resonance Signal. *Anal. Sens.*, *5*(4), e202400076.
6. Garcia, M. A. (2011). Surface plasmons in metallic nanoparticles: fundamentals and applications. *J. Phys. D: Appl. Phys.*, *28*, 283001.
7. Miller, M. E., & Shelby, J. E. (2010). Formation of cobalt nanocrystals in a borosilicate glass. *Phys. Chem. Glasses: Eur. J. Glass Sci. Technol.*, *B51*, 100-106.
8. Singla, S., Rajput, K., Kanjariya, P., Ravi, K., Anand, G., Kumar, N., Bansal, N. & Sharma, G. (2024). Structural, thermal, and optical properties of gold nanoparticle-doped bismuth borate glasses: effect of concentration. *J. Mater. Sci.: Mater. Electron.*, *35*(34), 2142.
9. Red'kov, A. V. (2012). Formation of composite materials based on glasses containing a reductant. *Phys. Solid State*, *54*, 1875.
10. Adamiv, V. T., Bolesta, I. M., Burak, Ya. V., Gamernyk, R. V., Karbovnyk, I. D., Kolych, I. I., Kovalchuk, M. G., Kushnir, O. O., Periv, M. V., & Teslyuk, I. M. (2014). Nonlinear optical properties of silver nanoparticles prepared in Ag doped borate glasses. *Physica B*, *449*, 31-35.
11. Dutka, R. M., Adamiv, V. T., Burak, Ya. V., Gamernyk, R. V., & Teslyuk, I. M. (2015). Preparation and nonlinear optical properties of $LiCaBO_3$-Ag_2O and $LiCaBO_3$-Gd_2O_3-Ag_2O borate glasses with Ag nanoparticles. *Phys. Status Solidi B*, *252*(12), 2745-2750.
12. Adamiv, V. T., Burak, Ya. V., Gamernyk, R. V., Dutka, R. M., & Teslyuk, I. M. (2014). Formation and Optical Properties of Ag Nanoparticles in CaB_4O_7–Ag_2O and CaB_4O_7–Gd_2O_3–Ag_2O Tetraborate Glasses. *J. Nano- and Electronic Physics*, *6*, 04033(7pp).
13. Adamiv, V. T., Burak, Ya. V., Gamernyk, R. V., Malynych, S. Z., Moroz, I. E., & Teslyuk, I. M. (2018). Optical nonlinearities in $LiKB_4O_7$–Ag_2O and $LiKB_4O_7$–Ag_2O–Gd_2O_3 glasses containing Ag nanoparticles, *Appl. Opt.*, *57*(17), 4802-4808.
14. Radaev, S., Muradyan, L., Malakhova, L., Burak, Ya., & Simonov, V. (1989). Atomic structure and electron density of lithium tetraborate $Li_2B_4O_7$. *Crystallogr. Reports*, *34*, 1400-1407.
15. Ono, Y., Nakaya, M., Kajitani T., Sugawara, T., Watanabe, N., Shiraishi, H., & Komatsu, R. (2000). Lithium potassium borate and lithium rubidium borate: new non-linear optical crystals. *Acta Cryst., C56*, 1413-1415.
16. König, H., & Hoppe, R. (1978). Über Borati der Alkalimetalle. II. Zur Kenntnis von LiB_3O_5 [1]. *Z. anorg. allg. Chem.*, *439*, 71.
17. Huppertz, H. (2003). β-CaB_4O_7: A New Polymorph Synthesized under High-Pressure/High-Temperature Conditions. *Z. Naturforsch.*, *58b*, 257-265.
18. Sastry, B. S. R., & Hummel, F. A. (1958). Studies in Lithium Oxide Systems: I. Li_2O, B_2O_3–B_2O_3. *J. Am. Ceram. Soc.*, *41*(1), 7–17.

19. Brant, A. T., Kananan, B. E., Murari, M. K., McClory, J. W., Petrosky, J. C., Adamiv, V. T., Burak, Ya. V., Dowben, P. A., & Halliburton, L. E. (2011). Electron and hole traps in Ag-doped lithium tetraborate ($Li_2B_4O_7$) crystals. *J. Appl. Phys*, *110*(9), 093719.
20. Adamiv, V. T., Burak, Ya. V., Girnyk, I. S., Kasperczyk, Ya., Kityk, I. V., & Teslyuk, I. M. (1997). The growth and properties of K- and Ag-doped $Li_2B_4O_7$ single crystals. *Functional Materials*, *4*(3), 415-418.
21. Adamiv, V., Kushlyk, M., Dutchak, U., Burak, Ya., Teslyuk, I., Medvid, I., Koflyuk, I., & Luchechko, A. (2025). Radiophotoluminescence in the Tissue-Equivalent LiB_3O_5:Ag Glasses. *Ukr. J. Phys. Opt.*, *26*(2), 02089 – 02096.
22. Fernández Navarro, J. M., Toudert, J., Rodríguez-Lazcano Y., Maté B., & Jiménez de Castro, M. (2013). Formation of sub-surface silver nanoparticles in silver-doped sodium–lead–germanate glass. *Appl. Phys. B*, *113*, 205-213.
23. Dmitruk, N. L., & Malinich, S. Z. (2014). Surface plasmon resonances and their manifestation in the optical properties of nanostructures of noble metals, *Ukr. J. Phys, 9*(1): *Reviews*, 3-37.
24. Obraztsov, P. A., Nashchekin, A. V., Nikonorov, N. V., Sidorov, A. I., Panfilova, A. V., & Brunkov, P. N. (2013). Formation of silver nanoparticles on the silicate glass surface after ion exchange. *Phys. Sol. State*, *55*(6), 1272–1278.
25. Adamiv, V., Teslyuk, I., Dyachok, Ya., Romanyuk, G., Krupych, O., Mys, O., Martynyuk-Lototska, I., Burak, Ya., & Vlokh, R. (2010). Synthesis and optical characterization of $LiKB_4O_7$, $Li_2B_6O_{10}$ and $LiCsB_6O_{10}$ glasses. *Applied Optics*, *49*(28), 5360-5365.
26. Henk, F. A. (2025). Mie scattering near the Fröhlich mode, *J. Opt. Soc. Am. A*, *42*, 580-586.
27. Johnson, P. B., & Christy, R. W. (1972). Optical Constants of the Noble Metals. *Phys. Rev. B*, *6*(12), 4370-4379.
28. Kaganovski, Yu., Mogilko, E., Lipovskii, A. A., & Rosenbluh, M. (2007). Formation of nanoclusters in silver-doped glasses in wet atmosphere. *J. Physics: Conference Serie*, *61*, 508-512.
29. Reintjes, J. F. (1984). *Nonlinear optical processes in liquids and gases*. Academic Press, Orlando.
30. Kelly, K. L., Coronado, E., Zhao, L. L. & Schatz, G. C. (2003). The Optical Properties of Metal Nanoparticles: The Influence of Size, Shape, and Dielectric Environment. *The Journal of Physical Chemistry B*, *107*, 668-677.
31. Malynych, S. & Chumanov, G. (2003). Light-Induced Coherent Interactions between Silver Nanoparticles in Two-Dimensional Arrays. *J. Am. Chem. Soc.*, *125*, 2896-2898.
32. Simo, A., Polte, J., Pfänder, N., Vainio, U., Emmerling, F., & Rademann, K. (2012). Formation mechanism of silver nanoparticles stabilized in glassy matrices. *J. Am. Chem. Soc.*, *134*, 18824−18833.
33. Paje, S. E., Llopis, J., Villegas, M. A., & Fernandez Navarro, J. M. (1996). Photoluminescence of a silver-doped glass. *Applied Physics A*, *63*, 431–434.
34. Bolesta, I. M., Borodchuk, A. V., Kushnir, A. A., Kolych, I. I., & Syworotka, I. I. (2011). Morphology and absorption spectra of ultra-thin films of silver. *Journal of Physical Studies*, *15*(4), 4703 (8 p.).

Adamiv, V. T., Burak, Ya. V., Teslyuk, I. M., Gamernyk, R. V., Horchynskyi, V. I., Yaremko, O. M. (2026). Optical and Morphological Features of Silver Species Formed in LiB_3O_5:Ag Glass by Thermal and Laser Treatment**.** *Ukrainian Journal of Physical Optics*, *27*(1), 01122 – 01131. doi: 10.3116/16091833/Ukr.J.Phys.Opt.2026. 01122

Анотація. *Досліджено морфологію та оптичні властивості наночастинок Ag (НЧ Ag) у зразках скла LiB_3O_5:Ag (0,1 мол.%), сформованих термічним відпалом на повітрі та у вакуумі, а також під впливом потужного лазерного випромінювання. Було виявлено, що основна маса НЧ Ag, сформованих термічним відпалом на повітрі, мають майже сферичну форму з R в діапазоні 20–100 нм, а значна частина поверхні зразків, відпалених у вакуумі, покрита НЧ Ag, сильно спотвореними відносно сферичної форми, з розмірами в діапазоні 100–200 нм, які перебувають в електричному контакті одна з одною. Лоренцеве розкладання записаних спектрів поглинання виявило 3-компонентні смуги поглинання – 241 нм, 367 нм та 426 нм, з яких лише одна смуга при 426 нм пов'язана з плазмонним резонансом на НЧ Ag, розташованих у приповерхневому шарі зразка, дві інші смуги при 241 нм та 367 нм пов'язані з іонами Ag^+ та агрегатами Ag_2^+ в об'ємі скла. Після обробки лазерним випромінюванням λ = 405 нм та потужністю 1,0 Вт, поверхня скляного зразка покривається несуцільною плівкою металевого Ag, над якою спостерігаються пластинчасті дендрити шириною 100–240 нм та довжиною 1–5 мкм, а в спектрі поглинання реєструються смуги при 368 нм та 820 нм, спричинені поверхневим плазмонним резонансом, причому перша смуга відповідає за несуцільну плівку Ag, тоді як друга, найімовірніше, пов'язана з дендритами металевого Ag.*

Ключові слова: *боратне скло, наночастинки Ag, плазмонний резонанс, LiB_3O_5:Ag*